https://doi.org/10.5194/amt-2021-354
Preprint. Discussion started: 29 October 2021

Atmospheric Measurement Techniques Discussions

Ozone Reactivity Measurement of Biogenic Volatile Organic Compound Emissions

Detlev Helmig[1,2*], Alex Guenther[3], Jacques Hueber[1], Ryan Daly[1], Wei Wang[1], Jeong-Hoo Park[1], Anssi Liikanen[4], Arnaud P. Praplan[4]

[1]Institute of Arctic and Alpine Research, University of Colorado, Boulder, CO 80309, USA
[2] now at: Boulder Atmosphere Innovation Research LLC, Boulder, CO 80305, USA
[3] University of California Irvine, CA, USA
[4]Atmospheric Research Composition, Finnish Meteorological Institute, 00101 Helsinki, Finland
***corresponding author: dh.bouldair@gmail.com**

Manuscript submitted to

Atmospheric Measurement Techniques

October 25, 2021

Abstract

Previous research on atmospheric chemistry in the forest environment has shown that the total reactivity by biogenic volatile organic compound (BVOC) emission is not well considered in forest chemistry models. One possible explanation for this discrepancy is the unawareness and neglect of reactive biogenic emission that have eluded common monitoring methods. This question motivated the development of a total ozone reactivity monitor (TORM) for the direct determination of the reactivity of foliage emissions. Emissions samples drawn from a vegetation branch enclosure experiment are mixed with a known and controlled amount of ozone (e.g. resulting in 100 ppb of ozone) and directed through a temperature-controlled glass flow reactor to allow reactive biogenic emissions to react with ozone during the approximately 2-minute residence time in the reactor. The ozone reactivity is determined from the difference in the ozone mole fraction before and after the reaction vessel. An inherent challenge of the experiment is the influence of changing water vapor in the sample air on the ozone signal. A commercial UV absorption ozone monitor was modified to directly determine the ozone differential with one instrument and sample air

https://doi.org/10.5194/amt-2021-354
Preprint. Discussion started: 29 October 2021


Atmospheric Measurement Techniques Discussions

was drawn through Nafion dryer membrane tubing. These two modifications significantly reduced errors associated with the determination of the reacted ozone compared to determining the difference from two individual measurements and errors from interferences from water vapor, resulting in a much improved and sensitive determination of the ozone reactivity. This paper provides a detailed description of the measurement design, the instrument apparatus, and its characterization. Examples and results from field deployments demonstrate the applicability and usefulness of the TORM.

1. Introduction

Recent field research on the atmospheric chemistry in forest environments has yielded a series of results that cannot be explained with our current comprehension of biogenic emissions, deposition processes, and chemical reactions. These findings date back to the pivotal paper by *Di Carlo et al.* [2004] that stimulated new interest and research into the question of unaccounted for biogenic volatile organic compound (BVOC) emissions. These researchers compared the directly measured hydroxyl radical (OH) reactivity in ambient air at the University of Michigan Biological Station (UMBS) PROPHET forest research site with the OH reactivity calculated from a comprehensive set of measured atmospheric gas phase species. The important conclusion of this study was that identified compounds could only account for about 2/3 of the directly measured OH reactivity. Interestingly, the difference between the two measurements, often called "missing OH reactivity" showed temperature dependence very similar to that found for monoterpene (MT) compounds. This similarity led the authors to hypothesize that the missing OH reactivity is due to non-identified BVOC emissions emitted from tree foliage at this site.

While these findings were surprising at the time of publication, several other subsequent studies have come to similar conclusions. OH reactivity measurements in ambient air have consistently shown higher OH reactivity values than what can be accounted for by quantified chemical species, and notably, the review of available measurements shows a tendency towards a

https://doi.org/10.5194/amt-2021-354
Preprint. Discussion started: 29 October 2021


Atmospheric Measurement Techniques Discussions

409 higher discrepancy at sites that are subjected to a relatively high influence from BVOC emissions
410 [*Lou et al.*, 2010].

411 The other line of research that has pointed towards the current underestimation of BVOC
412 emissions relies on ozone flux observation over forest canopies. *Kurpius and Goldstein* [2003]
413 segregated ozone deposition fluxes over a ponderosa pine plantation into stomatal uptake, non-
414 stomatal surface deposition, and gas phase chemistry contributions. They found that during sum-
415 mer, the ozone flux was dominated by gas-phase chemistry, and that the ozone loss showed an
416 exponential increase with temperature, with similar behavior as BVOC emissions. However, iden-
417 tified BVOCs could only account for a small fraction of this reactivity. Consequently, these re-
418 searchers postulated that there is a "large unrecognized source of reactive compounds in for-
419 ested environments". A follow-up study [*Goldstein et al.*, 2004], based on measurements during
420 a forest thinning experiment, went even further and claimed that "unmeasured BVOC emissions
421 are approximately 10 times the measured monoterpene flux". These hypotheses have been sup-
422 ported by findings from other subsequent studies [*Altimir et al.*, 2004; *Holzinger et al.*, 2005;
423 *Altimir et al.*, 2006; *Hogg et al.*, 2007; *Fares et al.*, 2010a; *Fares et al.*, 2010b; *Fares et al.*, 2010c;
424 *Wolfe et al.*, 2011].

425 There has been considerable progress in identifying and characterizing hitherto unrecog-
426 nized BVOC emissions. The most significant ones are light-dependent MT emissions [*Ortega et*
427 *al.*, 2007; *McKinney et al.*, 2011] and sesquiterpenes (SQT) [*Duhl et al.*, 2008]. Furthermore, it has
428 been recognized that methyl chavicol can be an important emission [*Bouvier-Brown et al.*, 2009a;
429 *Bouvier-Brown et al.*, 2009b; *Misztal et al.*, 2010]. However, inclusion of these emissions only
430 contributes a minor fraction to closing the gap between identified and inferred BVOC emissions.
431 In a study at the PROPHET site, using the comparative reactivity method, *Kim et al.* [2011] deter-
432 mined directly the OH reactivity in emission samples drawn from branch enclosures. OH reactivity
433 was also calculated based on BVOC emissions identified by Proton Transfer Reaction Mass Spec-
434 trometry (PTR-MS) and Gas Chromatography Mass Spectrometry (GC-MS). A red oak, white pine,
435 beech, and maple tree were investigated. Their results indicated a high range of total OH reac-
436 tivity from the emissions of these species, with red oak emissions showing the highest OH reac-

https://doi.org/10.5194/amt-2021-354
Preprint. Discussion started: 29 October 2021


Atmospheric Measurement Techniques Discussions

tivity overall. Identified isoprene and MT emissions could explain the directly measured OH reactivity from red oak, white pine, and beech. However, isoprene and monoterpene emissions from red maple could only explain a fraction of the measured OH reactivity. The OH reactivity from maple was dominated by emission of the SQT α-farnesene, which is a compound that would not have been identified in earlier studies of ambient BVOC at this site. These findings show that the chemical reactivity in emissions from different tree species can vary substantially in their overall magnitude and attribution to the emitted BVOC species. This indicates that there is the potential that ecosystems with different plant species composition could have substantial unaccounted for emissions that contribute to OH reactivity. This suggests that there must be BVOC compounds or compound classes emitted from foliage that current measurements do not capture, which is not unexpected given the major analytical challenges associated with analysis of some organic compounds.

In this work, we are describing a monitoring approach that addresses this dilemma by constraining the total ozone reactivity of BVOCs emissions with a direct measurement. These observations can be contrasted with the reactivity that is calculated from the sum of the reactivities of individual BVOCs and their OH reaction rates to assess the fraction of the identified and missing compounds that contribute to the total reactivity. The instrument relies on a flow reactor. Sample air containing BVOCs is mixed with a small flow containing a high mole fraction of ozone. The loss of ozone is monitored with a differential ozone measurement. Our Total Ozone Reactivity Monitor (TORM) that was previously presented in [*Helmig et al.*, 2010; *Park et al.*, 2013] has since undergone further testing and development. The calculation of ozone reactivity is explained in Supplement A, and the modelled decay of a few typically measured BVOC and ozone in the reactor is available in Supplement B.

Two other instruments relying on different types of reactor and detection methodology have been reported since [*Matsumoto*, 2014; *Sommariva et al.*, 2020]. These previous publications have also provided the principle and reaction kinetics consideration for this measurement. A linear double-tube Pyrex glass tube flow reactor with ozone detection up- and downstream of the reactor by two modified commercial (ECO PHYSICS, CLD770) chemiluminescence detectors (CLD)

https://doi.org/10.5194/amt-2021-354
Preprint. Discussion started: 29 October 2021


Atmospheric Measurement Techniques Discussions

was used in the work by *Matsumoto* [2014]. The ozone reactivity was determined from the difference of the two analyzers' signal. A 1 m long, 2.4 L volume-PTFE linear reactor was used by *Sommariva et al.* [2020]. These authors used two commercial Thermo Scientific Model 49i UV absorption monitors for the ozone determination, with the ozone reactivity again determined from the difference of the two monitor signals.

We particularly emphasize the necessity of properly characterizing the interference from water vapor on the ozone determination, and the advantage of the measurement of the amount of reacted ozone through a differential ozone determination with a single monitor. Thirdly, assembly of readily available instrument components facilitate a relatively easy, low expense instrument assembly.

Rigid chambers or flexible bag enclosures are the common approaches for studying biogenic emissions by dynamic or static vegetation enclosures [*Ortega and Helmig*, 2008; *Ortega et al.*, 2008]. Enclosure experiments allow the selective identification of emissions from individual plant species. Depending on the operational parameters, emissions can build up to many times, even order of magnitudes, higher levels than in ambient air. Higher temperatures (than in ambient air) are often encountered inside enclosures from the greenhouse warming effect, which enhances emissions and facilitates higher sensitivity of emissions determination. An inherent disadvantage and analytical challenge, however, is the evaporative water flux from the transpiring enclosed foliage. Under the most extreme, and not too uncommon conditions, water vapor saturation can be achieved inside the chamber, causing liquid water condensation on the chamber inside walls and within sampling tubing. The water flux is sensitive to the stomatal conductance, responding to conditions of light and temperature. In an ambient setting, these often change dynamically, causing similarly fast changes in water vapor concentration inside the enclosure and sample air. At 30^{o}C and water saturation, the water vapor mole fraction is approximately 4.2 %. A mere 10 % fluctuation equates to 4.2 parts per thousand, or 4,200,000 ppb of a water vapor change. The signals that have been achieved in ozone reactivity monitoring instruments system are usually in the single ppb range. Consequently, for the ozone monitoring to be selective, the ozone detection needs to be insensitive to water vapor changes that can be on the order of 10^{6}-10^{7} times

https://doi.org/10.5194/amt-2021-354
Preprint. Discussion started: 29 October 2021


Atmospheric Measurement Techniques Discussions

larger in mole fraction than the ozone signal. This is an enormous challenge for this measurement, as both the ozone CLD and UV absorption measurements are sensitive to water vapor.

Interference with an instrument signal response in the range of tens to hundreds of ppb has been reported for different types of UV absorption monitors from rapid changes in water vapor [*Wilson and Birks*, 2006; *Spicer et al.*, 2010]. This interference was traced to humidity effects on the transmission of light, i.e. reflectivity of light on the cell walls, through the optical cell [*Wilson and Birks*, 2006]. The study identified that the instrument's ozone scrubber amplified this effect, acting as a water reservoir adding or removing water to the air flow depending on the sample air moisture content. A 10 % change in the recorded ozone was observed from a 30 to 80 % RH increase for a UV absorption monitor [*Kim et al.*, 2019; *Kim et al.*, 2020]. Inserting a Nafion dryer into the sampling path can reduce the water interference, in the best scenario to within equal or better than ± 2 ppb [*Wilson and Birks*, 2006; *Spicer et al.*, 2010; *Kim et al.*, 2020]. *Sommariva et al.* [2020] found that the ozone wall losses were dependent on the relative humidity in their PTFE flow reactor.

While CLD analyzers for ozone determination are more expensive to acquire and operate, they are popular for fast ozone measurements such as for aircraft [*Ridley et al.*, 1992] and eddy covariance flux measurements [*Lenschow et al.*, 1981, 1982]. Similarly to UV monitors, CLD instruments suffer from an interference by water vapor, which in this case is caused by the quenching of the chemiluminescence signal in the reaction chamber [*Matthews et al.*, 1977; *Boylan et al.*, 2014]. A correction factor of 4-5 x 10^{-3} has been proposed, to be multiplied by the water vapor mole fraction in nmol mol^{-1} [*Boylan et al.*, 2014]. Under moist ambient air conditions, this correction can account for up to 15 % of the ozone signal. Consequently, following the enclosure system water vapor estimates above, CLD in an ozone reactivity system may be susceptible to a several percent interference from changing water vapor, which is on the same order of magnitude as the observed ozone reactivity observed in the flow chamber system.

Both, *Matsumoto* [2014] and *Sommariva et al.* [2020] used two ozone monitors for determination of the ozone upstream and downstream of the reactor, with the reacted ozone then determined as the difference of the recordings from both instruments. One objective of this con-

https://doi.org/10.5194/amt-2021-354
Preprint. Discussion started: 29 October 2021


Atmospheric Measurement Techniques Discussions

figuration in the *Matsumoto* [2014] work was to achieve a reduction of the quenching interference, based on the assumption that both monitors would have similar responses to the water interferences, with these errors then mostly cancelling out in the differential ozone reactivity signal calculation. From a measurement and signal perspective, this is a rather disadvantageous measurement approach for several reasons: (1) the two monitors need to be carefully synced/calibrated against each other to make sure the instrument offset is characterized and corrected for so that their readings are consistent; (2) drifts of any of the two monitors, or of both, will directly transfer to a measurement error in the ozone reactivity signal; and (3), statistically, the calculation of the ozone reactivity will be subject to a relatively large error, as the ozone reactivity signal is a relatively small value resulting from the difference between two larger numbers. Any absolute errors in the directly measured values will therefore transfer into a relatively large error of the smaller differential. For these reasons, it would be preferable to measure the ozone differential through a direct measurement with one monitor. Furthermore, a one monitor measurement would be advantageous in terms of instrument maintenance and cost.

Our experiment presented here overcomes this predicament by modifying a commercial UV absorption ozone monitor for the direct measurement of the ozone differential. Further, sample drying was implemented to reduce the aforementioned interference from fluctuations in the sample water vapor mole fraction. The experiments described here were conducted successively on two similar systems at the University of Colorado, Boulder, and the Finnish Meteorological Institute (FMI) in Helsinki, Finland.

2. Methods

The basic principle of the ozone reactivity determination of biogenic emissions is illustrated in Fig. 1. Emissions from vegetation are combined with a flow of ozone-enriched air and allowed to react in a flow reactor. Ozone is measured upstream and downstream of the reactor with a single instrument. In the standard configuration of an UV absorption ozone monitor, ozone-containing air and scrubbed air (ozone-free air) are either measured sequentially (one optical cell) or in

https://doi.org/10.5194/amt-2021-354
Preprint. Discussion started: 29 October 2021

Atmospheric Measurement Techniques Discussions

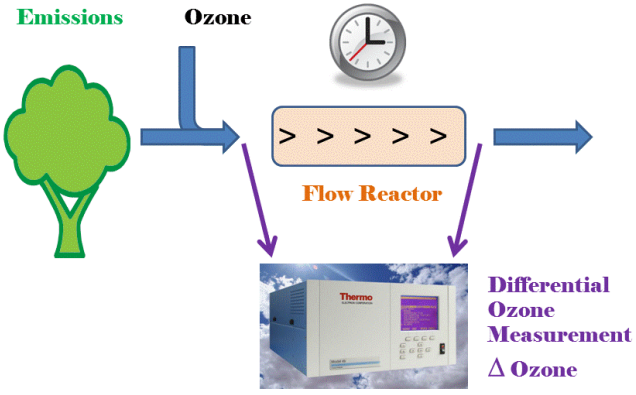

Figure 1
Principle of ozone reactivity measurement of biogenic emissions with one monitor that is configured for differential ozone signal recording.

parallel (two cell instruments), with the ozone mole fraction then determined following the Beer-Lambert Law. The ozone mole fraction is proportional to the natural logarithm of the light intensity *I* divided from the sample air (flow 1) by the light intensity in the scrubbed air I_o (flow 2). By replacing the scrubbed air flow path with a second sampling inlet line, the resulting signal no longer reflects the difference in ozone between the sample (1) and scrubbed air (2, zero ozone), but instead becomes the difference in ozone between the two sample flows (2-1). The required instrument modification is rather simple, illustrated in Fig. 2 for a Thermo Scientific Model 49i instrument. It requires removal of the ozone scrubber (MoO scrubber in most cases) and the separation of the scrubbed and sample air into two separate inlets. In the standard configuration, the 49i samples air at ≈ 1.2 L min^{-1} through one inlet. In the modified configuration, this flow is split in half to ≈ 0.6 L min^{-1} each for the Sample 1 and Sample 2 inlets. An early configuration of the experiment to illustrate how the differential ozone monitoring was evaluated against the monitoring of ozone up and downstream of the reactor with two instruments is presented in

https://doi.org/10.5194/amt-2021-354
Preprint. Discussion started: 29 October 2021

Atmospheric Measurement Techniques Discussions

(A) Original Pluming Configuration

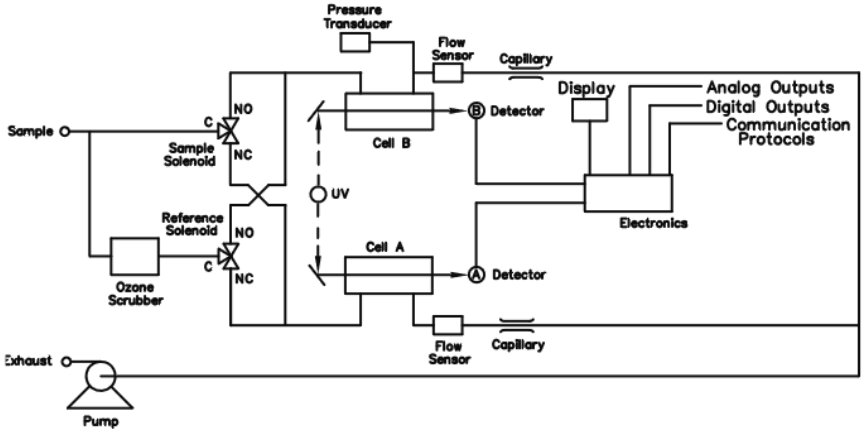

(B) Differential Ozone Monitoring Pluming Configuration

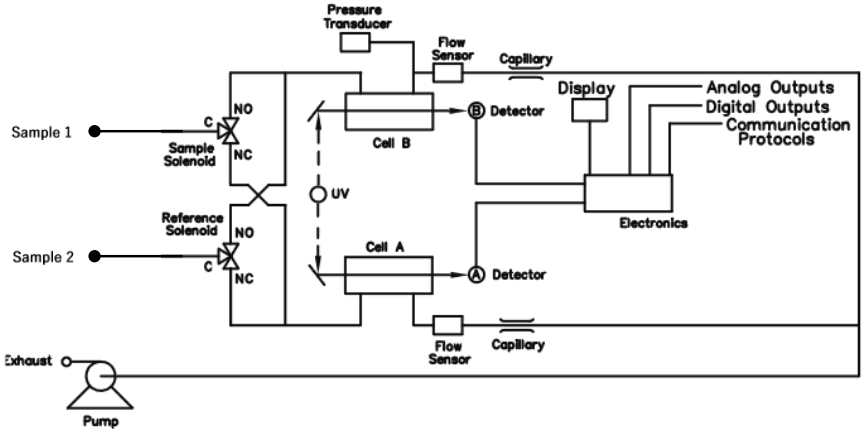

Figure 2
Plumbing configuration of a Thermo Scientific Instruments model 49 ozone UV absorption monitor in its original configuration (top) and in the modified configuration (bottom) for monitoring of ozone differentials.

564
565

https://doi.org/10.5194/amt-2021-354
Preprint. Discussion started: 29 October 2021


Atmospheric Measurement Techniques Discussions

Supplement C; the final one-monitor TORM configuration is shown in Fig. 3. The direct differential ozone measurement was always conducted with a Thermo Scientific Model 49i monitor. During the evaluation experiments, several different UV absorption ozone monitors were used for comparing the direct measurement with a result from two individual instruments. Those included Thermo Scientific Model 49i, Model 49C, and a MonitorLabs model 8810 monitor.

While other studies [*Matsumoto*, 2014; *Sommariva et al.*, 2020] utilized linear flow reactors, this experiment relied on using four glass flasks that were plumbed in series. The glass flask reactor design was chosen because it was deemed more compact and robust for field deployment applications. The 2.5 L borosilicate flasks that were used are air sampling flasks that are routinely deployed in the NOAA Cooperate Sampling Network for the global sampling of greenhouse gases. These glass flasks have been developed and extensively tested for their inertness and purity towards atmospheric trace gases (https://www.esrl.noaa.gov/gmd/ccgg/flask.html; flasks are fabricated by Allen Scientific, Boulder, CO). Flasks are covered with a protective film and have two ports with stopcock Teflon vales. One valve connects to a dip tube that leads to the inside on the opposite side of the flask (Fig. 4). This configuration allows efficient purging and replacement of the air volume inside the flasks with minimal mixing. The flasks were plumbed such that the inflowing air was always introduced through the dip tube. The four flasks in series add up to a total ≈10 L reactor volume. The flasks are contained in an 45 cm x 45 cm x 45 cm (inside dimension) Pelican model 0340 cube case (Torrance, CA) that was fitted with 5 cm foam insulation on the inside. A rope heater, temperature probe, and temperature controller allow to thermostatically control the temperature, typically to 40°C. The ozone reactant gas was provided from the Thermo Scientific 49i monitor using its integrated ozone generator. The output was set to provide a 1000 ppb constant output, so that the 1:10 dilution with the sample air flow resulted in a 100 ppb ozone mole fraction entering the reactor. All experiments described in this paper were conducted at this 100 ppb ozone mole fraction, unless stated otherwise. A mixer made of Teflon material (7.50 mm OD with 30 mixing elements, Stamixco AG, Wollerau, Switzerland) was inserted upstream of the introduction of the ozone gas flow for providing turbulent mixing between the sample air and ozone-enriched air. All tubing was made of 6.4 mm o.d./4.7 mm i.d. PFA tubing.

https://doi.org/10.5194/amt-2021-354
Preprint. Discussion started: 29 October 2021

Atmospheric Measurement Techniques Discussions

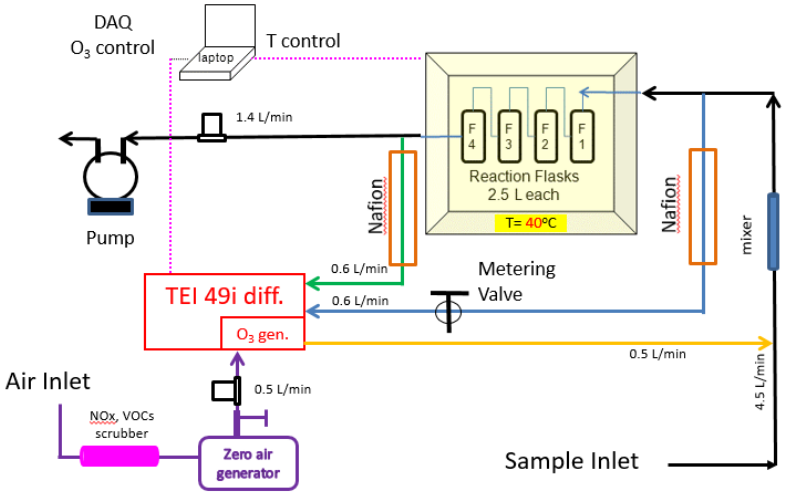

Figure 3
Final configuration of the total ozone reactivity monitor (TORM) using one Thermo Scientific (TEI) 49i PS monitor plumbed for the direct differential ozone measurement (Figure 2), and with the Nafion dryers and metering valve included. Flow rates are indicated in the figure. Total flow through the reactor is 5 L min^{-1}.

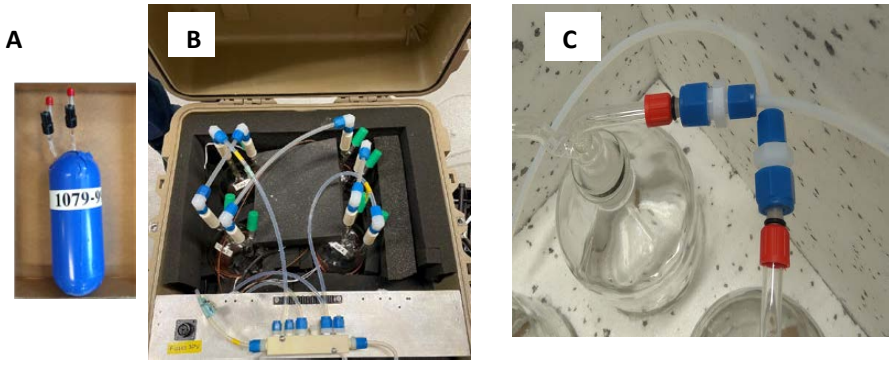

Figure 4
(A) Photograph of one of the glass flasks that were used for the University of Colorado, Boulder flow reactor. (B) The ozone reactor with four of the flasks plumbed in series contained in an insulated and temperature-controlled field-deployable enclosure. Four flasks were plumbed in series for a total flow reactor volume of 10 L. (C) The 2-L bottles (borosilicate glass 3.3) used in the Finnish flow reactor system.

https://doi.org/10.5194/amt-2021-354
Preprint. Discussion started: 29 October 2021


Atmospheric Measurement Techniques Discussions

599 Experiments did not consider adding an OH scavenger (i.e. cyclohexane) [*Matsumoto*, 2014;
600 *Sommariva et al.*, 2020]. *Sommariva et al.* [2020] estimated a < 6 % difference in ozone reactiv-
601 ity for BVOC ozonolysis reactions based on modeling, but could not identify differences with
602 and without cyclohexane added in their experiments. It is therefore unlikely that addition of an
603 ozone scrubber will make a notable difference in the ozone reactivity monitoring results. The
604 instrument operation and signal acquisition were controlled via a National Instruments digital
605 input interface and custom-written LabView software.

606 During field deployments, branch enclosures were set up on sweetgum (Liquidambar
607 styraciflua L.), white oak (Quercus alba), and loblolly pine (Pinus taeda) tree branches following
608 our previously described protocol [*Ortega and Helmig*, 2008]. A Tedlar bag (36"x24") was
609 wrapped around a tree branch of the size that when the bag is inflated, the branch was situated
610 in the middle of the bag with minimum touching of the wall. Scrubbed ambient air free of NO_x
611 ozone and BVOC (Purafil and activated charcoal scrubbers),was delivered to the enclosure at 25
612 L min^{-1}. Most of the moisture in the purge air was also removed by passing it through a set of
613 coils placed inside a refrigerator. The scrubber system did not remove carbon dioxide. Air sam-
614 ples from the enclosure were taken through the ports affixed on the Tedlar bag, drawn at flow
615 rates that are suitable for the sampling apparatus and instruments. The rest of the purge air es-
616 caped the enclosure mainly through the gap between the bag and the main stem of the branch.
617
618

619 # 3. Results and Discussion

620

621 ### 3.1 System conditioning

622 A newly assembled system exhibited a significant ozone sink, on the order of 20-30 ppb loss
623 of ozone (at 100 ppb) at a 5 L min^{-1} reactor flow. The slow decline of the ozone loss signal over
624 time indicated a gradual equilibration of the system to the ozone in the sample air. This ozone
625 loss and signal drift could almost entirely be eliminated thorough conditioning of all tubing and
626 the reactor with an air flow enriched in ozone. For this conditioning, the system was purged for
627 24 hours with 500 ppb of ozone. After this treatment, the ozone loss associated with the sample

https://doi.org/10.5194/amt-2021-354
Preprint. Discussion started: 29 October 2021


Atmospheric Measurement Techniques Discussions

flow through the reactor in the absence of chemical gas reactants, i.e. the reactor background signal, was, depending on the particular system condition and operational variables, on the order of 1-2 % of the supplied ozone mole fractions; i.e. at 100 ppb ozone, the loss was reduced to 1-2 ppb and did no longer show any drifts in the signal. After warmup, the 1-min averaged $\Delta[O_3]$ signal displayed a standard deviation (σ) of 0.075 - 0.096 ppb (over 1 h, n = 60). This translates into a limit of detection (3σ) of 1.8 – 2.3 x 10^{-5} s^{-1} for the reactivity (for a theoretical residence time of 150 s, and correcting for the ozone dilution flow). This sensitivity is slightly higher, i.e. resulting in a lower limit of detection than that reported by [*Matsumoto*, 2014] (4 x 10^{-5} s^{-1}, for a residence time of 57 s), and approximately 2-3 times lower than that reported by [*Sommariva et al.*, 2020] (4.5– 9 x 10^{-5} s^{-1} for a residence time of 140 s). The stability of the ozone reactivity signal was tested on the Finnish system over a full daily cycle of changing ambient conditions in temperature, humidity, and light. There was no notable drift in the $\Delta[O_3]$ signal over the measurement period despite the changes in the environmental conditions (Supplement D).

3.2 Balancing of the ozone monitor inlet pressures

The readings from the differential ozone monitor are sensitive to the difference in the pressure in the two sampling lines that connect to upstream and downstream of the reactor (Supplement E). The pressure differential results from the vacuum generated by the sampling pump for providing flow through the reactor. The 49i diagnostics menu allows monitoring of the pressures of the two optical cells. In the original configuration, it was found that there was a pressure difference of, depending of the flow rate, 20-30 torr between the two cells at a 5 L min^{-1} reactor flow, with the lower pressure recorded in the line downstream of the reactor. This pressure differential alters between negative and positive values as the monitor alternates air from the two inlets through the two optical cells. This pressure difference results in an artificial ozone signal offset between the two sampling paths. An increase of the flow rate through the reactor causes a change in the pressure difference and the ozone differential reported by the monitor: Increasing the flow rate from 2 to 9 L min^{-1} corresponded to an increase from 2 to 7 ppb increase in the

https://doi.org/10.5194/amt-2021-354
Preprint. Discussion started: 29 October 2021


Atmospheric Measurement Techniques Discussions

656 differential ozone signal. This behavior is clearly a measurement artifact and counter to the ex-
657 pected ozone loss, as the actual chemical ozone loss decreases with decreasing residence time
658 of the air inside the reactor (i.e. increasing flow rate). This measurement artifact was mitigated
659 by inserting a 0.64 cm Teflon metering valve into the sampling line upstream of the reactor. By
660 closing the valve slightly, the flow was restricted to where both cell pressure readings from the
661 reactor were equal (within ≈1 torr). This resulted in an ozone differential signal of ≈1.7 ppb that
662 was insensitive to the reactor flow rate (Supplement E). The final plumbing configuration of the
663 TORM and its integration into a vegetation enclosure experiment is shown in Fig. 5.
664
665 **3.3 Evaluation of the direct differential ozone reactivity measurement**

666 Results from the parallel operation of two ozone monitors measuring the actual ozone be-
667 fore and after the reactor, with Δ[O3] calculated from the difference of the two readings, com-
668 pared to the direct ozone differential measurement by TORM are summarized in Fig. 6. Field data,
669 collected during the Southern Oxidant and Aerosol Study (SOAS) (CU Boulder system), constitute
670 a total of ten days of measurements collected using branch enclosures on three different
671 branches of sweetgum trees. The ozone differential was normalized to the air flow through the
672 chamber and to the dried weight of leaf biomass that was sampled from the vegetation in the
673 branch enclosure. These time series data show a clear diurnal cycle with the ozone reactivity
674 increasing steeply during daytime hours. Results are reasonably consistent between days and the
675 three different enclosures, considering that the BVOCs emissions that determine this signal are
676 highly sensitive to light and the enclosure temperature, which varied during the experiment.
677 There is high agreement between the ozone reactivity results from both configurations across
678 these experiments. A linear regression between results from the two monitoring methods from
679 the SOAS study yields a slope value of 0.996. The graphed data also show the substantial im-
680 provement in the noise of the measurement with the direct differential monitoring (A, B). The
681 precision error of the direct differential measurement is only about 1/5 compared to the result
682 from the two monitors. After the system equilibration, the 1-σ standard deviation of the differ-
683 ential ozone measurement for 1-min averaged readings was generally in the range of

https://doi.org/10.5194/amt-2021-354
Preprint. Discussion started: 29 October 2021

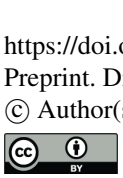

Atmospheric Measurement Techniques Discussions

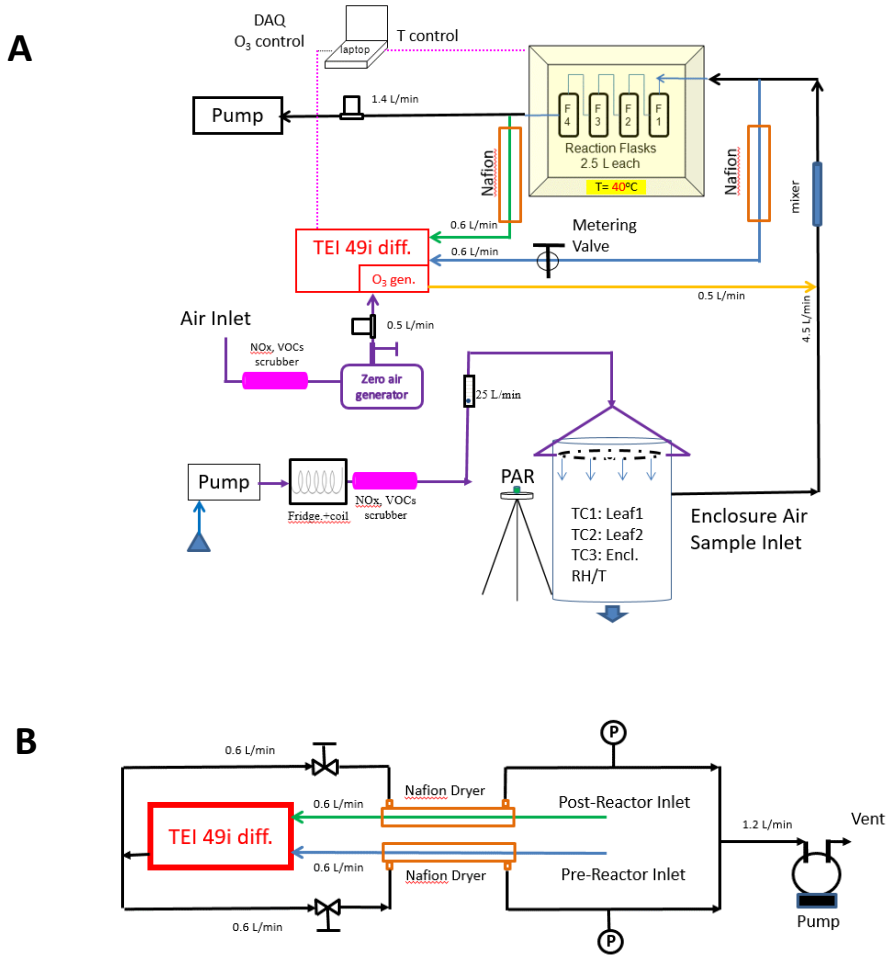

Figure 5
(A) Final configuration of the total ozone reactivity monitor with one differential ozone monitor, the sampling line pressure balancing valve, and the Nafion dryers. Schematic (B) shows the detail of the Nafion Dryer plumbing including the external pump that was added to the system for providing the purge flow for the Nafion dryers.

684

https://doi.org/10.5194/amt-2021-354
Preprint. Discussion started: 29 October 2021

Atmospheric Measurement Techniques Discussions

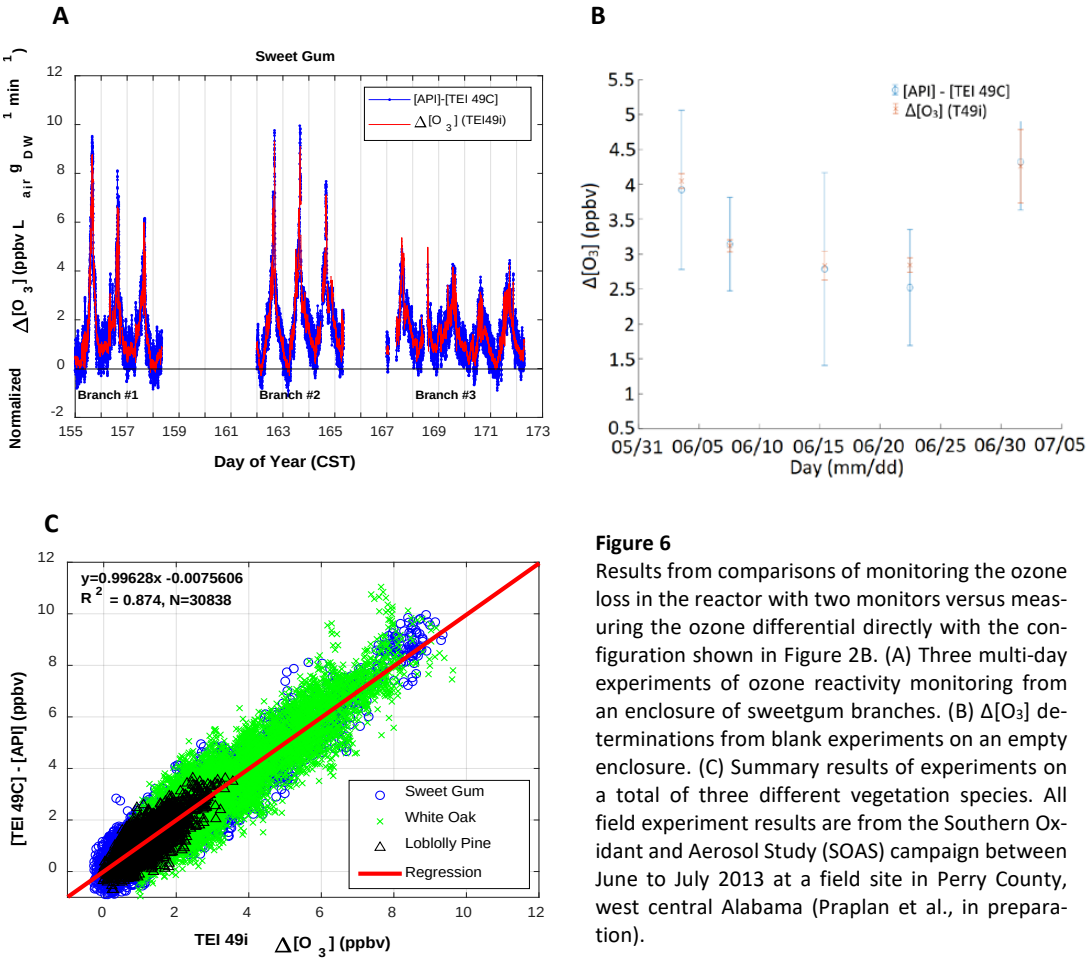

Figure 6
Results from comparisons of monitoring the ozone loss in the reactor with two monitors versus measuring the ozone differential directly with the configuration shown in Figure 2B. (A) Three multi-day experiments of ozone reactivity monitoring from an enclosure of sweetgum branches. (B) $\Delta[O_3]$ determinations from blank experiments on an empty enclosure. (C) Summary results of experiments on a total of three different vegetation species. All field experiment results are from the Southern Oxidant and Aerosol Study (SOAS) campaign between June to July 2013 at a field site in Perry County, west central Alabama (Praplan et al., in preparation).

0.1 – 0.2 ppb, which was 2-3 times lower than the calculated ozone difference from the two-monitor measurement. These results clearly indicate the benefits of the single monitor measurement: (1) the accuracy of the ozone reactivity measurement is consistent with the differential two-monitor determination; (2) there is a very significant improvement in the measurement precision from using a single monitor; and (3) the operation of a single monitor is less tedious and labor intensive as it does not require the regular intercomparison for determination of offsets

https://doi.org/10.5194/amt-2021-354
Preprint. Discussion started: 29 October 2021


Atmospheric Measurement Techniques Discussions

692 and drifts and correction algorithms for calibrating the response of two individual monitors
693 [*Bocquet et al.*, 2011; *Sommariva et al.*, 2020].
694
695 **3.4 Sample residence time in the reactor**
696
697 The desired operation of a flow reactor system is for air to move through the reactor as a
698 narrow plug, with minimal turbulence and mixing. Most flow reactors are tubular and linear and
699 are used in laboratory settings. Depending on their operational variables, they achieve seconds
700 to a few minutes residence time. The residence time and peak broadening during transport
701 through the reactor was studied by installing a syringe injection port upstream of the reactor,
702 injection of a small volume of a 1 ppm standard of nitric oxide (NO), and monitoring the ozone
703 loss from the ozone + NO reaction downstream of the reactor with a fast-response (5 Hz) nitric
704 oxide chemiluminescence instrument. Experiments were conducted in two different configura-
705 tions: 1. In the normal plumbing configuration, with the incoming air introduced to each flask
706 through the dip tube. 2. To test the effect of the dip tube, the plumbing was also reversed. The
707 flow through the reactor was set to 4 L min^{-1}, which for an ideal flow reactor, at 10 L volume,
708 should result in a 2.4 min (150 s) residence time. Results of these tests are shown in Fig. 7. For
709 both configurations, the peak signal was observed earlier than the theoretical time, i.e. ≈30 s for
710 the normal configuration, and ≈50 s for the reversed configuration. The peak widths (at half of
711 peak maximum) were ≈90 s and 120 s, for the normal and reversed configuration, respectively.
712 The behavior in these data show that there is a considerable amount of mixing inside the reactor
713 glass flasks, causing deviation from an ideal flow reactor. Nonetheless, the residence time of ≈120
714 s for the normal plumbing configuration is sufficient to meet the requirements for the ozone
715 reaction experiment. The findings from this experiment were confirmed at a higher, 6 L min^{-1}
716 flow rate (Supplement F). Both experiments show the advantage of the air introduction through
717 the dip tube, resulting in a narrower peak, i.e. narrower defined residence time.

https://doi.org/10.5194/amt-2021-354
Preprint. Discussion started: 29 October 2021

Atmospheric Measurement Techniques Discussions

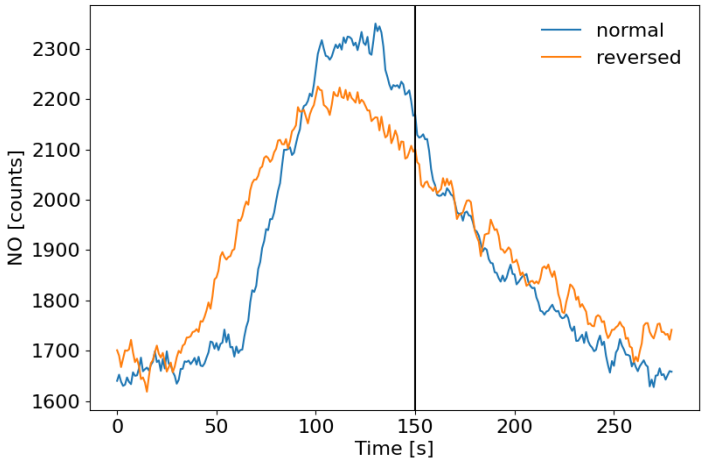

Figure 7
Test of sample air residence time in the flow reactor. A small volume of a 1 ppm NO standard was injected through a port upstream of the reactor and NO was monitored downstream with a fast response chemiluminescence analyzer (1 s time resolution). 5 s running averages are presented here. The normal configuration was with the flow entering each flask through the dip tube. The reversed configuration was with the air low exiting each flask through the dip tube. The vertical black line indicates the theoretical residence time based on the total flow rate (4 L min^{-1}) and total volume (10 L) of the reactor, assuming that there was no mixing inside the flasks.

3.5 Evaluation and Mitigation of Humidity effects

As elucidated on in the introduction section, changes in humidity can severely interfere in the ozone determination. Ozone monitors have been found to be less sensitive, i.e. report ozone below its actual value at high humidity, and to exhibit large artificial signal fluctuations from rapid changes in the sample water vapor. Characterization and mediation of the sensitivity of the ozone reactivity measurement to water vapor was a main emphasis of our experiments. Earlier experiments, where the sampling flow was subjected to variable water vapor, such as by injecting small volumes of water through an injection port upstream of the reactor in the configuration shown in Supplement C, confirmed the findings from prior literature: Despite a constant ozone mole fraction that was fed into the reactor, both, the two-monitor determination, and the single monitor ozone differential determination, showed instantaneous changes in the ozone signal, reaching on the order of 10 ppb. The bias in the ozone recording lasted significantly longer (≈10 times)

https://doi.org/10.5194/amt-2021-354
Preprint. Discussion started: 29 October 2021


Atmospheric Measurement Techniques Discussions

than the residence time that was determined in the above described experiment using nitric oxide. These water vapor effects on the ozone signal were mitigated by two modifications to the TORM: (1) the glass flasks reactor was insulated and a heater, regulated by a temperature controller was added to control the temperature of the reactor to 40°C. This heating significantly reduced the residence and interference time from the water injection, likely due to a reduction of the adherence of the water vapor to the walls of the glass flasks and other reactor components. Our observations agree with the findings reported by *Wilson and Birks* [2006], who found a reduction of the water interference for their 2B Technologies ozone monitor when the glass optical cell was slightly heated; and (2) Nafion dryers (0.64 cm o.d. x 180 cm length; MD-110-72 gas dryer, Perma Pure LLC, New Jersey, USA) were inserted into both ozone monitor inlet flows before and after the reactor. We installed the two Nafion dryers there, rather than one Nafion dryer for the sample flow path going into the reactor, to prevent possible losses of polar and unsaturated compounds from the sample flow passing through a Nafon dryer, as has been reported in other prior research. The purge flow for the Nafion dryers was provided by the vent flow from the TEI 49i. The analyzer vent flow was split into two approximately equal fractions, resulting in 0.6 L min^{-1} flow for each Nafion Dryer (Figure 5B). Throttle valves were installed in both lines as flow restrictors and adjusted such that the pressure in the exterior chamber of the Nafion dryers was ≈10 % below the interior section of the dryer (cell pressure readings from the differential 49i monitor). The Nafion dryers were conditioned using the same protocol as for the reactor (see above), after which there was no notable ozone loss from sampling the ozone-enriched air flow through the Nafion tubing, in agreement with other previous studies that have reported negligible ozone loss in Nafion tubing materials [*Wilson and Birks*, 2006; *Boylan et al.*, 2014; *Kim et al.*, 2020].

Results from an experiment with the Nafion dryers in use and where water vapor was increased in multiple steps is shown in Fig. 8. The same humidification system as described by *Boylan et al.* [2014] was used for moisturizing a zero air dilution gas fed to the TORM. The resulting humidity was recorded with a LICOR model 7000 CO_2/H_2O gas analyzer downstream of the mixer, but upstream of the reactor. Each humidity level was maintained for 30 min, before subjecting the system to the next higher moisture level by a rapid change in the humidity generator

https://doi.org/10.5194/amt-2021-354
Preprint. Discussion started: 29 October 2021

Atmospheric Measurement Techniques Discussions

setpoint. The ozone reactivity signal was monitored with the differential 49i monitor, as well as by recording the absolute ozone upstream and downstream of the reactor with two individual monitors. Both ozone monitoring systems were sampling through the Nafion tubing. Results of the experiment (Fig. 8) show a residual ozone reactivity signal response of ≈0.5 ppb over an ≈10 to 84 % RH span for the differential monitor. The two-monitor $\Delta[O_3]$ response is approximately six times as large. The spikes seen during the moisture transition periods seen in earlier experiments disappeared completely for the differential monitor.

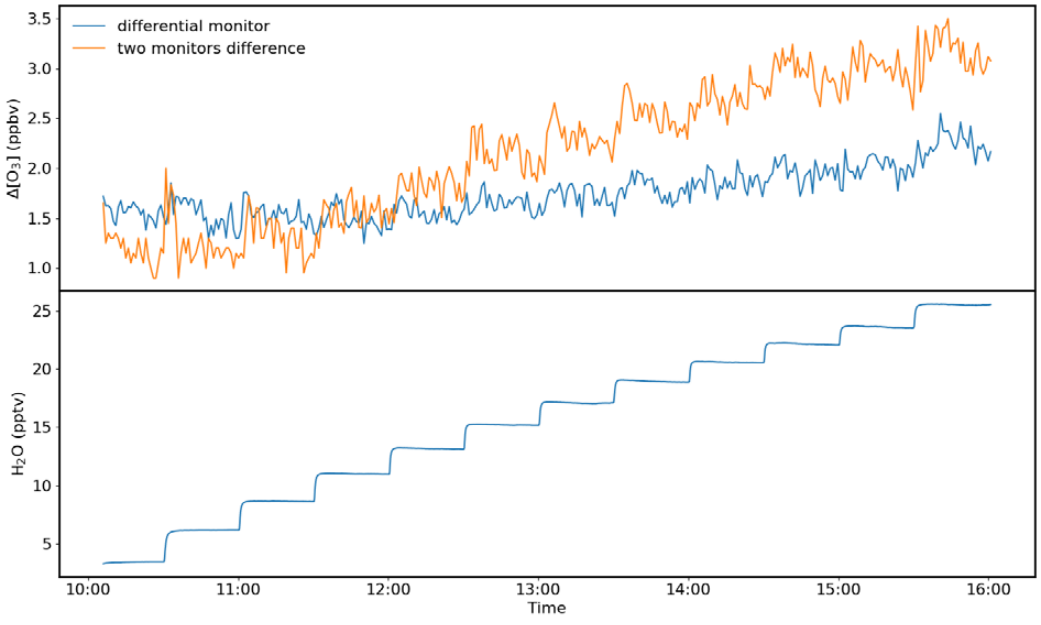

Figure 8
Experiment with increasing humidity in the air supplied to the TORM. The humidity content of the sample air is displayed in the lower graph in units of parts per thousand (ppt). A total of 12 levels were administered, from ≈3 -26 ppt, which at room temperature conditions (25°C) is approximately equivalent to a RH range of 10-84 %.

Similar order of magnitude results were obtained in a series of experiments where liquid water (20 to 100 µl) was injected into the sampling flow through a septum port upstream of the reactor. The Nafion dryer removed ≈2/3 of the water interference, and the differential monitor response to the water injection was less than half compared to calculated difference from the two-monitors configuration (Supplement G).

https://doi.org/10.5194/amt-2021-354
Preprint. Discussion started: 29 October 2021

Atmospheric Measurement Techniques Discussions

774 **3.6 Application Examples**
775
776 Ozone reactivity of test mixtures and samples from vegetation enclosures were investigated
777 in laboratory and field systems. A laboratory experiment using a flow of limonene standard is
778 presented in Fig. 9. The gas standard was prepared in house for a target mole fraction of 20 ppm.
779 However, the actual mole fraction is expected to have decreased with time, but could not be
780 independently verified at the time of the experiment. The reported mole fractions, after mixing
781 of the standard with the dilution flow, range between 0 -33 ppbv, which is a typical range
782

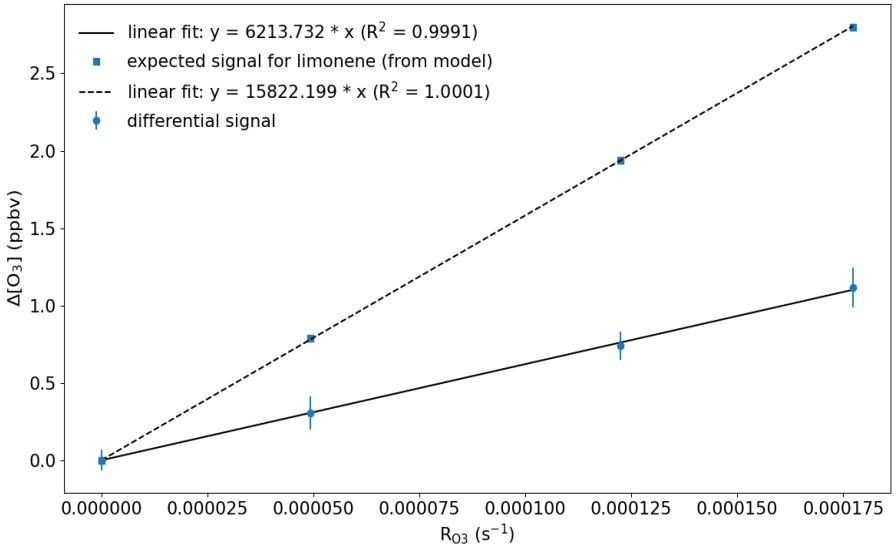

Figure 9
Laboratory test of the TORM. A small flow of a high mole fraction limonene standard was fed into the system upstream of the reactor. The theoretical reactivity calculated from the BVOC ozone rate constant, ozone mole fraction, and residence time are given on the x-axis. Error bars represent the standard deviation for the monitoring data at each level.

783
784 observed during enclosure experiments) and represents upper limit values for the mole fraction.
785 The TORM determination shows good linearity, with a R^2 result of the linear regression of 0.9991.
786 At the highest limonene level, the TORM signal, recorded with the differential ozone monitor,
787 was 0.9 ppb (after subtraction of the 1.7 ppb Δ ozone reactor background that was determined
788 for this particular application).

https://doi.org/10.5194/amt-2021-354
Preprint. Discussion started: 29 October 2021


Atmospheric Measurement Techniques Discussions

In Fig. 9, the experimental results from the limonene experiments are also compared with the modeled signal for various O_3 reactivity values for limonene for the operating conditions of TORM during this experiment. The modeled results reflect the expected O_3 decrease due to the reaction with limonene after the reaction corresponding to the theoretical residence time in the reactor (here 167 s; 3.6 l min^{-1} flow through a 10 L reactor). The applied rate constant for the reaction of ozone with limonene at 298 K is 21 x 10^{-17} cm^3 s^{-1} [*Atkinson and Arey*, 2003]. A linear regression shows that $\Delta[O_3]$ is linearly dependent with RO_3 (ca. 1.5 ppbv/(10^{-4} s^{-1})). The discrepancy between the model and the experiment stem likely from the uncertainty of the mixing ratio in the limonene standard. The experimentally determined sensitivity, i.e. approximately 0.5 ppbv/(10^{-4} s^{-1}), is therefore a lower limit. Applying a lower limonene mole fraction in the standard would lead to a proportionally higher value.

The TORM has been deployed in field settings at several research sites in the U.S. and in Finland. Fig. 10 displays results from one of these field experiments, i.e. a 3-day branch enclosure experiment on a red oak tree at the University of Michigan Biological Station. These data show results from the 2nd and 3rd days of the experiment. The experiment was conducted on relatively warm and sunny days as can be seen in the radiation and temperature data. Besides the ozone reactivity signal, shown in panel A, the figure also includes the concurrent measurements of photochemical active radiation (PAR) (B), respiration and photosynthesis (C), and leaf and enclosure temperature (D). The change in humidity, reaching a maximum of on the order of 25 parts per thousand as the mid-day maximum when foliage respiration peaks, confirms our estimate presented in the introduction section for the humidity changes during vegetation enclosure experiments. Emission samples collected from this enclosure and analyzed by gas-chromatography showed that emissions from this branch were dominated by isoprene, with further substantial emissions of MT and SQT compounds. On both days, the TORM recorded a mid-day maximum differential ozone signal of 12-14 ppb, dropping to 2-3 ppb at night. The instrument readings are quite similar on both days. The ozone reactivity clearly follows a daily cycle, with low values during nighttime hours, and daytime maxima during the early afternoon. The ozone reactivity signal

https://doi.org/10.5194/amt-2021-354
Preprint. Discussion started: 29 October 2021

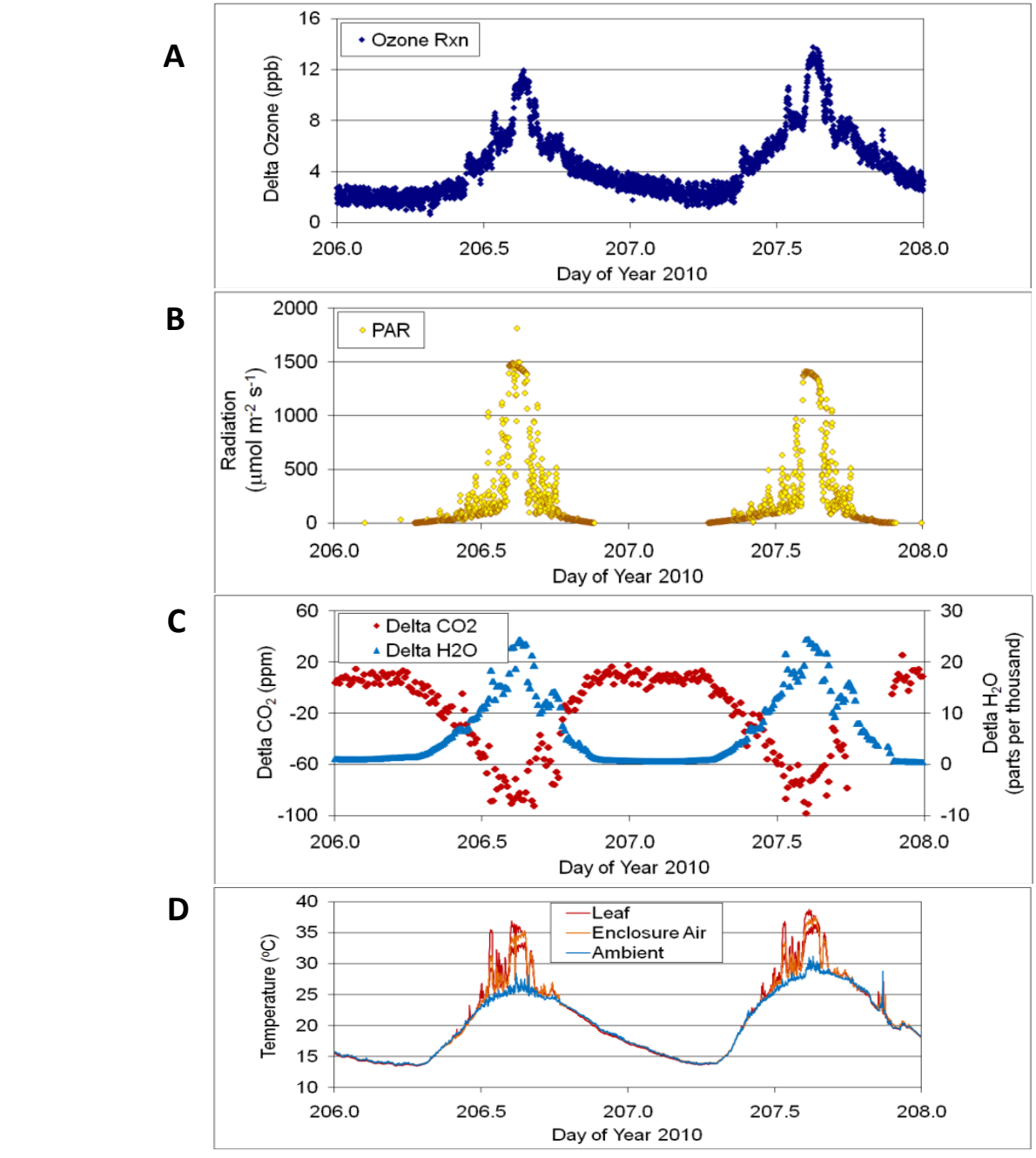

Figure 10
Results obtained over two days from a branch enclosure experiment on a red oak tree, with data for the ozone reactivity measurement (A), solar radiation (B), respiration and photosynthesis expressed as the difference in the water and CO_2 mole fractions in the air stream going into and out of the enclosure (C), and leaf, inside enclosure, and ambient temperature (D).

https://doi.org/10.5194/amt-2021-354
Preprint. Discussion started: 29 October 2021


Atmospheric Measurement Techniques Discussions

817 maxima coincide with the peak in diurnal radiation, respiration, and photosynthesis, which sug-
818 gests that the ozone-reactive emissions are modulated by light availability. Comparison of the
819 observed ozone reactivity with the calculated ozone reactivity from identified BVOC species could
820 only account for a fraction of the observed reactivity (*Praplan et al., manuscript in preparation*).
821 Similar diurnal cycles of ozone reactivity were observed for sweetgum in the Southern Oxidant
822 and Aerosol Study [*Park et al.*, 2013], as can be seen in the ten days of measurements shown in
823 Fig. 5. Please note that the data in Fig. 5 were normalized to the leaf dry mass of the enclosure
824 foliage.

825 A presentation of the ozone reactivity results normalized to the leaf dry mass and as a func-
826 tion of leaf temperature for experiments performed at UMBS is shown in Fig. 11. All four species
827 show an increase of reactivity with increasing temperature. This feature indicates that all species
828 emit reactive volatiles at increasing rates as temperature increases. Interestingly, the normalized
829 reactivity is quite different, varying by at least a factor of three. It also appears that the temper-
830 ature dependencies are different, with red maple showing a more dynamic increase than other
831 species. Remarkably, white pine, a high MT emitter, gave the lowest reactivity results. Further-
832 more, red maple results appear to be higher than for red oak, despite the fact that red oak was
833 found to emit high amounts of BVOC, totaling ≈100 x those of maple, but with most of the emis-
834 sions made up by isoprene. The relatively high levels of ozone reactivity are also noteworthy in
835 light of the independent OH reactivity study by *Kim et al.* [2011], who found that red maple emis-
836 sions exhibited the highest missing OH reactivity associated with SQT in comparison with these
837 other three species. Consequently, red maple is a prime candidate for having reactive BVOC emis-
838 sions that hitherto have not been chemically identified.

https://doi.org/10.5194/amt-2021-354
Preprint. Discussion started: 29 October 2021

Atmospheric Measurement Techniques Discussions

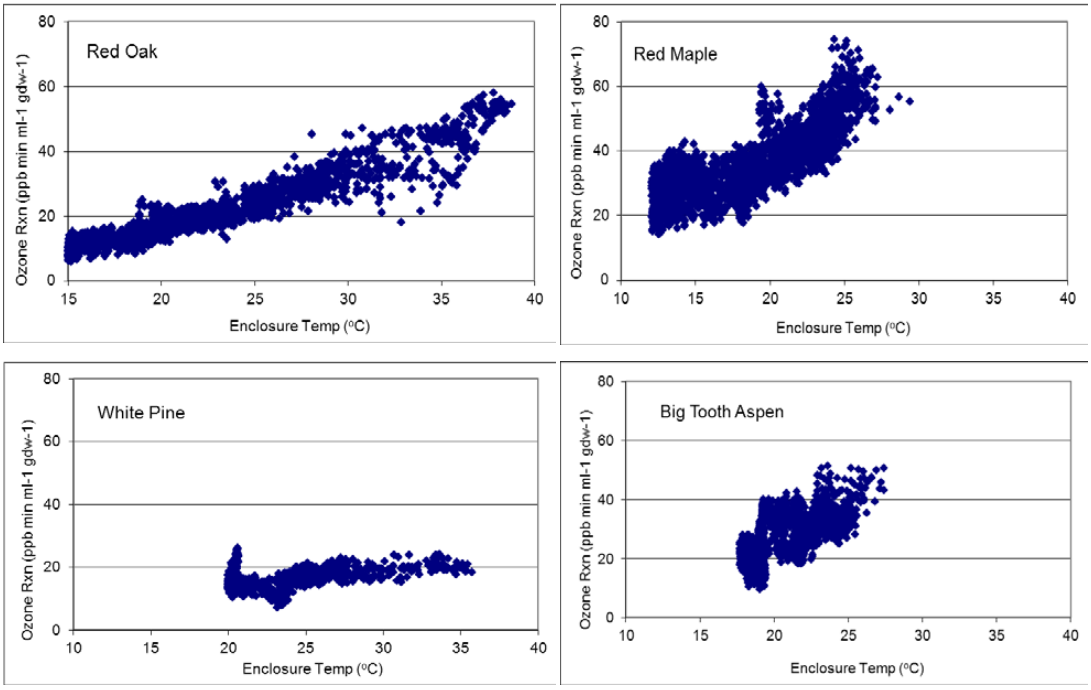

Figure 11
Ozone reactivity results from experiments on red oak, red maple, white pine, and big tooth aspen, normalized to the amount of leaf dry mass and flow rate, as a function of enclosure temperature.

4. Summary and Conclusions

A total ozone reactivity monitor, TORM, was developed for the study of the ozone reactivity of biogenic emissions. TORM builds on standard laboratory equipment and can be assembled with moderate technically skilled personnel and at relatively moderate cost. The instrument was thoroughly characterized, and a number of ameliorations were implemented that significantly improved the measurement sensitivity and reduced the interference from absolute and changing water vapor in the sample air. Critical improvements over previously reported measurement approaches were the adaptation of a commercial ozone UV absorption monitor for direct measurement of the reacted ozone (ozone differential), heating and temperature control of the reactor, and the drying of the sample flows with Nafion dryers. Specific challenges arose with this setup

https://doi.org/10.5194/amt-2021-354
Preprint. Discussion started: 29 October 2021


Atmospheric Measurement Techniques Discussions

that could be overcome, such as balancing the pressure difference for each cell in the differential ozone monitor (one cell measuring before the reactor and the other cell measuring after).

TORM has been used in a number of field settings and proven the feasibility and value of this new measurement. Ozone reactivity signals on the order of 5-0 ppb have been obtained in enclosure experiments on high-BVOC emitting species. These signals are 20-50 times above the noise level of the measurement. Chemical identification of BVOC emissions from the enclosure and estimation of the total reactivity of identified emissions has been able to only account for a fraction of the directly measured ozone reactivity. Detailed description of these field studies and discussion of the results, including the attribution of the directly measured ozone reactivity to identified BVOC emissions, will be presented in a forthcoming publication (*Praplan et al., in preparation*).

Data availability

All data that the work builds on are presented in the manuscript and Supplemental Information.

Disclaimer

This study does not necessarily reflect the views of the funding agencies, and no official endorsements should be inferred.

Funding Information

The development and testing of the TORM system has been made possible through funding from the U.S. National Science Foundation, grants #AGS 0904139, ATM-1140571, and AGS-1561755, as well as funding from the Academy of Finland (decisions nos. 307797 and 314099).

Author contribution

D.H. Principal Investigator of the U.S. study, managed research grants, oversaw the study, prepared and approved the manuscript.

A.G. Co-Principal Investigator of the U.S. study, reviewed and approved the manuscript.

J.H. Constructed instrumentation and conducted experiments, developed control and data acquisition software, approved the manuscript.

R.D. Constructed instrumentation and conducted experiments, participated in field studies, reviewed and approved the manuscript.

https://doi.org/10.5194/amt-2021-354
Preprint. Discussion started: 29 October 2021

W.W. Constructed instrumentation, conducted experiments, prepared, reviewed, and approved the manuscript.

J.H.P. Constructed instrumentation, developed instrument control software, conducted lab and field experiments, reviewed and approved the manuscript.

A.L. Constructed instrumentation, conducted lab and field experiments, approved the manuscript.

A.P.P. Principal Investigator of the Finnish study, conducted field and lab experiments, prepared and approved the manuscript.

Competing Interests

The authors declare that they have no conflict of interest.

References

Altimir, N., P. Kolari, J. P. Tuovinen, T. Vesala, J. Back, T. Suni, M. Kulmala, and P. Hari (2006), Foliage surface ozone deposition: a role for surface moisture?, *Biogeosciences*, *3*, 209-228.

Altimir, N., J. P. Tuovinen, T. Vesala, M. Kulmala, and P. Hari (2004), Measurements of ozone removal by Scots pine shoots: calibration of a stomatal uptake model including the non-stomatal component, *Atmospheric Environment*, *38*, 2387-2398, doi:10.1016/j.atmosenv.2003.09.077.

Atkinson, R., and J. Arey (2003), Gas-phase tropospheric chemistry of biogenic volatile organic compounds: a review, *Atmospheric Environment*, *37*, S197-S219, doi:10.1016/s1352-2310(03)00391-1.

Bocquet, F., D. Helmig, B. A. Van Dam, and C. W. Fairall (2011), Evaluation of the flux gradient technique for measurement of ozone surface fluxes over snowpack at Summit, Greenland, *Atmospheric Measurement Techniques*, *4*, 2305-2321, doi:10.5194/amt-4-2305-2011.

Bouvier-Brown, N. C., A. H. Goldstein, D. R. Worton, D. M. Matross, J. B. Gilman, W. C. Kuster, D. Welsh-Bon, C. Warneke, J. A. de Gouw, T. M. Cahill, and R. Holzinger (2009a), Methyl chavicol: characterization of its biogenic emission rate, abundance, and oxidation products in the atmosphere, *Atmospheric Chemistry and Physics*, *9*, 2061-2074.

Bouvier-Brown, N. C., R. Holzinger, K. Palitzsch, and A. H. Goldstein (2009b), Large emissions of sesquiterpenes and methyl chavicol quantified from branch enclosure measurements, *Atmospheric Environment*, *43*, 389-401, doi:10.1016/j.atmosenv.2008.08.039.

Boylan, P., D. Helmig, and J. H. Park (2014), Characterization and mitigation of water vapor effects in the measurement of ozone by chemiluminescence with nitric oxide, *Atmospheric Measurement Techniques*, *7*, 1231-1244, doi:10.5194/amt-7-1231-2014.

Di Carlo, P., W. H. Brune, M. Martinez, H. Harder, R. Lesher, X. R. Ren, T. Thornberry, M. A. Carroll, V. Young, P. B. Shepson, D. Riemer, E. Apel, and C. Campbell (2004), Missing OH reactivity in a forest: Evidence for unknown reactive biogenic VOCs, *Science*, *304*, 722-725.

Duhl, T. R., D. Helmig, and A. Guenther (2008), Sesquiterpene emissions from vegetation: a review, *Biogeosciences*, *5*, 761-777.

Fares, S., A. Goldstein, and F. Loreto (2010a), Determinants of ozone fluxes and metrics for ozone risk assessment in plants, *Journal of Experimental Botany*, *61*, 629-633, doi:10.1093/jxb/erp336.

https://doi.org/10.5194/amt-2021-354
Preprint. Discussion started: 29 October 2021

Atmospheric Measurement Techniques Discussions

Fares, S., M. McKay, R. Holzinger, and A. H. Goldstein (2010b), Ozone fluxes in a Pinus ponderosa ecosystem are dominated by non-stomatal processes: Evidence from long-term continuous measurements, *Agricultural and Forest Meteorology*, *150*, 420-431.

Fares, S., J. H. Park, E. Ormeno, D. R. Gentner, M. McKay, F. Loreto, J. Karlik, and A. H. Goldstein (2010c), Ozone uptake by citrus trees exposed to a range of ozone concentrations, *Atmospheric Environment*, *44*, 3404-3412, doi:10.1016/j.atmosenv.2010.06.010.

Goldstein, A. H., M. McKay, M. R. Kurpius, G. W. Schade, A. Lee, R. Holzinger, and R. A. Rasmussen (2004), Forest thinning experiment confirms ozone deposition to forest canopy is dominated by reaction with biogenic VOCs, *Geophysical Research Letters*, *31*, doi:L22106

10.1029/2004gl021259.

Helmig, D., R. Daly, and S. B. Bertman (2010), Ozone reactivity of biogenic volatile organic compounds from four dominant tree species at PROPHET-CABINEX, *Abstract A53C-0240, 2010 Fall Meeting, AGU, San Francisco, Calif., 13-17 Dec.* .

Hogg, A., J. Uddling, D. Ellsworth, M. A. Carroll, S. Pressley, B. Lamb, and C. Vogel (2007), Stomatal and non-stomatal fluxes of ozone to a northern mixed hardwood forest, *Tellus Series B-Chemical and Physical Meteorology*, *59*, 514-525, doi:10.1111/j.1600-0889.2007.00269.x.

Holzinger, R., A. Lee, K. T. Paw, and A. H. Goldstein (2005), Observations of oxidation products above a forest imply biogenic emissions of very reactive compounds, *Atmospheric Chemistry and Physics*, *5*, 67-75.

Kim, D. J., T. V. Dinh, J. Y. Lee, I. Y. Choi, D. J. Son, I. Y. Kim, Y. Sunwoo, and J. C. Kim (2019), Effects of Water Removal Devices on Ambient Inorganic Air Pollutant Measurements, *International journal of environmental research and public health*, *16*, 9, doi:10.3390/ijerph16183446.

Kim, D. J., T. V. Dinh, J. Y. Lee, D. J. Son, and J. C. Kim (2020), Effect of Nafion Dryer and Cooler on Ambient Air Pollutant (O-3, SO2, CO) Measurement, *Asian J. Atmos. Environ.*, *14*, 28-34, doi:10.5572/ajae.2020.14.1.028.

Kim, S., A. Guenther, T. Karl, and J. Greenberg (2011), Branch-level measurement of total OH reactivity for constraining unknown BVOC emission during CABINEX (Community Atmosphere-Biosphere INteractions Experiments)-09 field campaign, *Atmos. Chem. Phys. Discuss.*, *11*, 7781-7809.

Kurpius, M. R., and A. H. Goldstein (2003), Gas-phase chemistry dominates O-3 loss to a forest, implying a source of aerosols and hydroxyl radicals to the atmosphere, *Geophysical Research Letters*, *30*, doi:1371

10.1029/2002gl016785.

Lenschow, D. H., R. Pearson, and B. B. Stankov (1981), Estimating the ozone budget in the boundary-layer by use of aircraft measurements of ozoneeddy flux and mean concentration, *Journal of Geophysical Research-Oceans*, *86*, 7291-7297, doi:10.1029/JC086iC08p07291.

Lenschow, D. H., R. Pearson, and B. B. Stankov (1982), Measurements of ozone vertical flux to ocean and forest, *Journal of Geophysical Research-Oceans and Atmospheres*, *87*, 8833-8837, doi:10.1029/JC087iC11p08833.

Lou, S., F. Holland, F. Rohrer, K. Lu, B. Bohn, T. Brauers, C. C. Chang, H. Fuchs, R. Haseler, K. Kita, Y. Kondo, X. Li, M. Shao, L. Zeng, A. Wahner, Y. Zhang, W. Wang, and A. Hofzumahaus (2010), Atmospheric OH reactivities in the Pearl River Delta - China in summer 2006: measurement and model results, *Atmospheric Chemistry and Physics*, *10*, 11243-11260, doi:10.5194/acp-10-11243-2010.

Matsumoto, J. (2014), Measuring Biogenic Volatile Organic Compounds (BVOCs) from Vegetation in Terms of Ozone Reactivity, *Aerosol Air Qual. Res.*, *14*, 197-206, doi:10.4209/aaqr.2012.10.0275.

Matthews, R. D., R. F. Sawyer, and R. W. Schefer (1977), Interferences in chemiluminescence measurement of NO and NO2 emissions from combustion systems, *Environ. Sci. Technol.*, *11*, 1092-1096.

McKinney, K. A., B. H. Lee, A. Vasta, T. V. Pho, and J. W. Munger (2011), Emissions fo isoprenoids and oxygenated biogenic volatile organic compounds from a New England mixed forest, *Atmos. Chem. Phys.*, *11*, 4807-4831.

https://doi.org/10.5194/amt-2021-354
Preprint. Discussion started: 29 October 2021

970 Misztal, P. K., S. M. Owen, A. B. Guenther, R. Rasmussen, C. Geron, P. Harley, G. J. Phillips, A. Ryan, D. P. Edwards, C.
971 N. Hewitt, E. Nemitz, J. Siong, M. R. Heal, and J. N. Cape (2010), Large estragole fluxes from oil palms in Borneo,
972 *Atmospheric Chemistry and Physics*, *10*, 4343-4358, doi:10.5194/acp-10-4343-2010.

973 Ortega, J., and D. Helmig (2008), Approaches for quantifying reactive and low-volatility biogenic organic compound
974 emissions by vegetation enclosure techniques - Part A, *Chemosphere*, *72*, 343-364,
975 doi:10.1016/j.chemosphere.2007.11.020.

976 Ortega, J., D. Helmig, R. W. Daly, D. M. Tanner, A. B. Guenther, and J. D. Herrick (2008), Approaches for quantifying
977 reactive and low-volatility biogenic organic compound emissions by vegetation enclosure techniques - Part B:
978 Applications, *Chemosphere*, *72*, 365-380, doi:10.1016/j.chemosphere.2008.02.054.

979 Ortega, J., D. Helmig, A. Guenther, P. Harley, S. Pressley, and C. Vogel (2007), Flux estimates and OH reaction
980 potential of reactive biogenic volatile organic compounds (BVOCs) from a mixed northern hardwood forest,
981 *Atmospheric Environment*, *41*, 5479-5495, doi:10.1016/j.atmosenv.2006.12.033.

982 Park, J., A. B. Guenther, and D. Helmig (2013), Ozone reactivity of biogenic volatile organic compound (BVOC)
983 emissions during the Southeast Oxidant and Aerosol Study (SOAS), in *American Geophysical Union, Fall Meeting*
984 *2013, abstract #A13A-0172*, edited.

985 Ridley, B. A., F. E. Grahek, and J. G. Walega (1992), A small, high-sensitivity, medium-response ozone detector
986 suitable for measurements from light aircraft, *Journal of Atmospheric and Oceanic Technology*, *9*, 142-148,
987 doi:10.1175/1520-0426(1992)009<0142:ashsmr>2.0.co;2.

988 Sommariva, R., L. J. Kramer, L. R. Crilley, M. S. Alam, and W. J. Bloss (2020), An instrument for in situ measurement
989 of total ozone reactivity, *Atmospheric Measurement Techniques*, *13*, 1655-1670, doi:10.5194/amt-13-1655-2020.

990 Spicer, C. W., D. W. Joseph, and W. M. Ollison (2010), A Re-Examination of Ambient Air Ozone Monitor Interferences,
991 *Journal of the Air & Waste Management Association*, *60*, 1353-1364, doi:10.3155/1047-3289.60.11.1353.

992 Wilson, K. L., and J. W. Birks (2006), Mechanism and elimination of a water vapor interference in the measurement
993 of ozone by UV absorbance, *Environmental Science & Technology*, *40*, 6361-6367, doi:10.1021/es052590c.

994 Wolfe, G. M., J. A. Thornton, W. A. McKay, and A. H. Goldstein (2011), Forest-atmosphere exchange of ozone:
995 Sensitivity to very reactive biogenic VOC emissions and implications for in-canopy photochemistry, *Atmos. Chem.*
996 *Phys. Discuss.*, *11*, 13381-13424.